Geophys. J. R. astr. Soc. (1975) **41**, 81–105.

Analysis to Extended Periods of Rayleigh and Love Wave Dispersion across Australia

John H. Goncz, Anton L. Hales and Kenneth J. Muirhead

(Received 1974 November 14)*

Summary

Group velocities and phase velocities for Rayleigh waves and Love waves have been measured to periods of almost 200 s for nine paths across Australia. This extended range of dispersion data was obtained by the new process of summing cross-correlograms of a large number of seismograms of earthquakes with moderate magnitudes (average m_b was 5.8) prior to the non-linear computation of phase. This is an unbiased averaging process that enhances the signal at longer periods. Western–central Australia has the same dispersion as shield areas of other parts of the world; eastern Australia may be catalogued tectonic or 'aseismic platform'. Group velocity for eastern Australian paths has a pronounced minimum value, possibly less than 3·4 km s^{-1}, between 100- and 200-s period. Smoothed Rayleigh wave phase velocities were obtained by integration of regionally averaged group velocity curves. A usable estimate of fundamental mode Love wave phase velocities was obtained by Fourier analysis of sums of cross-correlograms, but Love wave group velocities could not be resolved by frequency-time analysis.

Introduction

The variations in dispersion of surface waves across the Australian continent have been previously investigated by Bolt & Niazi (1964) and by Thomas (1969). These early studies of the Rayleigh wave phase velocities were restricted to periods of less than 50 s and consequently do not provide information about the shear velocities at depths greater than 40 km. There is apparently no Love wave dispersion data for the Australian continent reported in the literature.

In order to examine the shear velocity structure of the upper mantle to greater depths by inversion of surface wave dispersion, the range of dispersion data must extend to periods longer than 50 s. However, the analysis of a single surface wave observation is usually limited by a deteriorating signal–noise ratio at the longer periods. A method for enhancing the signal–noise ratio at longer periods for the two-station method is needed. Such a method has been suggested by Dziewonski & Hales (1972), who observed that the cross-correlation operation performed on two seismograms of a two-station pair 'normalizes' the data with respect to the path

* Received in original form 1974 August 29.

between the two stations. The phase spectrum of the cross-correlogram, except for perturbation by noise, depends only on the interstation distance and the dispersive properties of the medium between the two stations. Thus, an arbitrary number of cross-correlograms, derived from an ensemble of earthquakes whose epicentres lie near the great circle path defined by the locations of the two stations, can be summed before performing the non-linear operation required to calculate the phase spectrum. Some of the sources of noise contamination of long period records are:

(1) refraction at continental boundaries causing later arrival of energy at either or both stations;

(2) multi-path propagation or reflection from continental boundaries;

(3) multiple or extended source functions in time and space that generate overlapping wave trains;

(4) higher mode propagation;

(5) contamination by body waves; for example, core reflections can arrive in the midst of a dispersed surface wave train;

(6) seismic and instrumental background noise, significant in the low-amplitude portions of the signal spectrum.

All of these interfering noises, except (6) are event generated and can therefore be randomized by taking events from different distances and from opposite directions. If the noise is uncorrelated among the events and the phase spectra are invariant, it is obvious that signal enhancement will be obtained by stacking cross-correlograms. While it is true that any individual event may have a considerable amount of signal-organized noise associated with it, the inclusion of events with varying epicentral distances tends to disorganize this noise with respect to the phase spectrum contained in the sum of cross-correlograms. This paper reports the results of a surface wave study of the Australian continent in which these new ideas were used to successfully extend the period range of analysis.

Data acquisition and processing

The five WWSSN stations in Australia make available nine intra-continental paths for study. Thomas's (1969) list of 35 earthquakes was used as a basis for this investigation, but early results indicated that more events would have to be included in the sums of cross-correlograms in order to achieve sufficient signal enhancement. A computer search of events catalogued since 1963 was conducted to find earthquakes with epicentres within 6° of the appropriate great circle and with a magnitude greater than $5{\cdot}5\,m_b$.

A complete list of the earthquakes used in this study appears in Table 1. Identification numbers up to 40 correspond with Thomas's (1969) identification numbers, those above 100 represent additional events.

Phase velocities were computed by the equation

$$c(T) = \frac{D_{12}}{t_2 - t_1 + T\left(\dfrac{\phi_2(T) - \phi_1(T) + m}{2\pi}\right)} \tag{1}$$

where t_2 and t_1 are Greenwich Mean Time at the start of the digitized seismograms for station 2 and station 1, T is period, $\phi_2(T)$ and $\phi_1(T)$ are phase angles in radians and m is an integer reflecting the ambiguity associated with the periodicity of trigonometric functions. A computer program was written which finds, by search and trial,

Table 1

Identification number	Day	Mon	Yr	Hr	Min	Sec	Path	Epicentre	M_b	Deviation from great circle(°)	% Path length error	(R)ayleigh or (L)ove
34	16	3	1965	16	46	15.5	CTA to TAU	40.80 N 142.90 E	5.6	0.9	0.4	L
102	23	10	1965	8	33	47.4	TAU to CTA	55.00 S 146.20 E	5.7	5.6	0.0	RL
1	25	12	1962	12	9	45.6	TAU to ADE	36.20 S 100.20 W		6.3	0.2	R
8	18	5	1963	12	20	31.9	ADE to TAU	8.20 S 115.60 E	5.9	6.3	0.7	R
11	15	6	1963	15	30	37.7	TAU to ADE	36.30 S 98.90 W	4.9	5.5	0.0	R
18	24	9	1963	16	30	16.0	TAU to ADE	10.60 S 78.00 W	6.5	6.2	0.1	R
112	3	11	1965	1	39	3.1	TAU to ADE	9.10 S 71.40 W	6.2	1.0	0.5	L
113	12	10	1966	0	6	38.8	ADE to TAU	12.00 S 121.70 E	5.6	0.5	0.2	R
119	13	8	1970	4	22	38.5	ADE to TAU	8.89 S 117.98 E	6.0	3.4	0.3	RL
120	24	8	1970	12	30	19.5	TAU to ADE	56.59 S 142.48 W	5.9	4.0	0.0	R
39	28	3	1963	23	29	14.6	ADE to MUN	9.60 S 177.50 W	5.1	0.6	0.0	RL
38	31	3	1963	19	22	53.3	ADE to MUN	30.00 S 178.00 W	6.0	2.0	0.0	R
3	28	3	1963	11	12	31.3	ADE to MUN	30.20 S 177.80 W		2.4	0.0	R
6	2	4	1963	4	43	30.9	ADE to MUN	29.70 S 177.10 W		1.9	0.0	RL
13	14	7	1963	0	2	22.8	ADE to MUN	30.50 S 177.20 W	5.3	3.1	0.1	R
20	4	10	1963	2	47	32.1	ADE to MUN	20.70 S 174.00 W	5.3	8.8	0.8	R
24	31	10	1963	3	17	42.0	ADE to MUN	21.80 S 175.00 W	6.3	8.0	0.7	R
124	9	12	1965	6	7	47.7	ADE to MUN	17.30 N 100.00 W	6.0	0.2	0.1	RL
128	5	4	1969	2	18	29.9	MUN to ADE	12.15 N 41.20 E	6.2	3.1	0.2	RL
129	4	2	1970	5	8	48.0	ADE to MUN	15.53 N 99.48 W	6.0	2.3	0.0	RL
130	25	10	1970	12	0	35.2	MUN to ADE	13.69 S 66.26 E	5.8	5.2	0.4	RL
7	13	5	1963	22	48	10.3	CTA to ADE	6.00 S 150.10 E		7.2	0.5	R
9	2	6	1963	10	0	0.1	CTA to ADE	6.10 S 154.50 E	5.7	8.4	0.7	RL
12	24	6	1963	16	17	15.4	CTA to ADE	52.30 N 171.20 W	5.4	2.2	0.5	R
19	2	10	1963	3	31	27.0	CTA to ADE	5.40 S 152.00 E	5.6	1.0	0.1	R
21	26	10	1963	22	41	29.8	CTA to ADE	5.20 S 152.00 E	5.9	1.2	0.2	L
136	22	7	1968	5	9	15.7	ADE to CTA	54.62 S 1.74 E	5.6	2.6	0.3	RL
40	28	3	1963	23	29	14.6	RIV to MUN	19.60 S 177.50 W	5.1	12.8	1.4	RL
37	31	3	1963	19	22	53.3	RIV to MUN	30.00 S 178.00 W	6.0	6.4	0.3	RL
36	4	10	1963	2	47	32.1	RIV to MUN	20.70 S 174.00 W	5.3	7.8	0.5	R
141	17	5	1964	19	26	20.6	MUN to RIV	35.20 N 35.90 W	5.6	2.3	-	L
144	2	3	1965	9	19	41.6	RIV to MUN	27.20 S 177.90 W	5.6	0.6	0.0	R
145	27	12	1967	16	22	48.5	RIV to MUN	22.30 S 174.80 W	6.1	5.9	0.3	RL
147	5	4	1969	2	18	29.9	MUN to RIV	12.15 N 41.20 E	6.2	5.1	0.4	RL
149	25	10	1970	12	0	35.2	MUN to RIV	13.69 S 66.26 E	5.8	3.2	0.1	R
4	28	3	1963	23	29	14.6	RIV to ADE	29.60 S 177.50 W	5.1	9.4	1.0	R
5	31	3	1963	19	22	53.3	RIV to ADE	30.00 S 178.00 W	6.0	10.0	1.1	R
15	13	8	1963	21	52	37.4	RIV to ADE	19.30 S 173.70 W	5.1	6.1	0.5	R
16	14	8	1963	2	46	44.1	RIV to ADE	21.40 S 175.20 W	4.7	4.1	0.2	R
22	27	10	1963	10	38	49.0	RIV to ADE	22.80 S 175.20 W	4.8	1.8	0.1	R
152	21	7	1965	2	51	39.0	RIV to ADE	20.90 S 175.70 W	5.7	5.4	0.4	RL
154	9	12	1965	6	7	47.7	RIV to ADE	17.30 N 100.00 W	6.0	5.0	0.5	RL
159	25	10	1970	12	0	35.2	ADE to RIV	13.69 S 66.26 E	5.8	1.2	0.0	RL
160	27	6	1965	9	45	48.7	TAU to RIV	54.70 S 5.20 E	5.9	1.8	0.4	R
161	17	7	1965	7	20	30.7	RIV to TAU	9.70 S 159.80 E	6.4	3.0	0.3	R
163	16	8	1965	12	36	23.6	TAU to RIV	0.50 S 19.90 W	6.2	1.3	0.8	L
164	19	10	1966	8	1	33.8	TAU to RIV	1.50 S 15.40 W	6.2	4.4	0.4	L
165	22	7	1968	5	9	15.7	TAU to RIV	54.62 S 1.74 E	5.6	0.0	0.5	RL
166	18	8	1968	18	38	30.6	RIV to TAU	10.11 S 159.86 E	6.2	3.5	0.3	L
167	26	11	1968	0	3	14.3	TAU to RIV	57.53 S 6.79 W	5.6	5.7	0.0	RL
168	31	10	1969	11	33	4.8	RIV to TAU	51.32 N 179.01 W	6.0	0.9	0.5	RL
169	25	6	1970	5	13	58.6	RIV to TAU	7.92 S 158.69 E	6.1	0.5	0.2	RL
170	17	6	1963	18	30	54.3	RIV to CTA	65.70 S 179.30 W	5.6	1.2	0.2	RL
33	30	12	1964	13	19	47.4	RIV to CTA	62.60 S 165.80 E	5.2	5.5	0.1	RL
171	24	8	1965	14	3	16.0	CTA to RIV	3.20 S 141.00 E	5.5	1.0	0.2	L
175	26	5	1968	14	41	52.0	RIV to CTA	63.34 S 170.70 E	5.5	2.3	0.1	RL
176	21	4	1969	7	19	27.5	CTA to RIV	32.19 N 131.86 E	6.1	1.5	0.3	R
178	29	6	1969	17	9	13.9	RIV to CTA	62.78 S 166.27 E	5.5	5.2	0.1	R
28	20	8	1964	12	48	47.7	MUN to CTA	37.40 S 78.30 E		4.1	0.0	RL
181	17	2	1966	11	47	56.8	MUN to CTA	32.20 S 78.90 E	6.4	5.9	0.2	RL
184	10	7	1968	11	16	44.6	MUN to CTA	36.81 S 78.54 E	5.7	2.9	0.0	RL
187	22	10	1969	22	51	33.5	CTA to MUN	34.83 N 121.34 W	5.9	2.6	0.4	R

the value for m at each Fourier interval which (1) gives the smoothest phase velocity curve, and (2) has a geophysically suitable value at the longest period.

D_{12} is the great circle distance between the two stations. If the epicentre does not lie precisely on this great circle, D_{12} in equation (1) should be replaced by the difference between the two epicentral distances $D_2 - D_1$ (Thomas 1969). However, for events with great circle deviations of less than 6° this correction, which is a func-

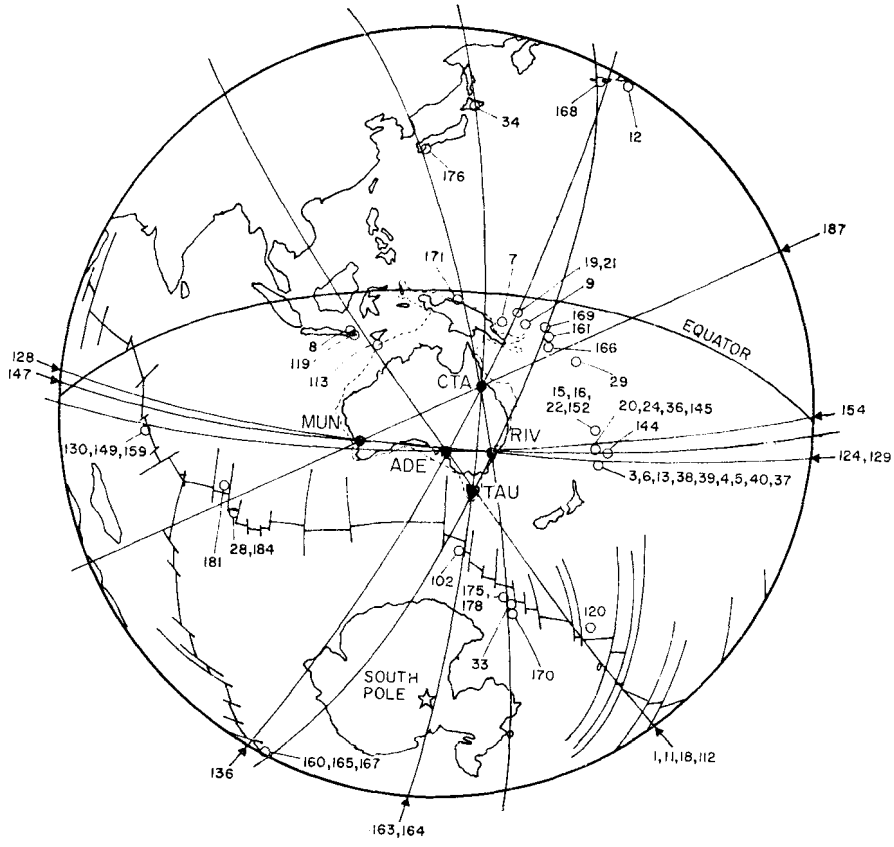

FIG. 1. Stereographic world projection showing locations of earthquakes and seismic stations used in this study.

tion of both epicentral distance as well as the deviation from the great circle path, is small as can be seen from the penultimate column of Table 1. When the correction is small the summation of cross-correlograms does not introduce significant error.

The stereographic world projection centred on Australia in Fig. 1 shows the locations of the five WWSSN stations and also the events used in this study.

It is of computational interest to point out that this study was accomplished entirely on a PDP–15 mini-computer with programs capable of fitting in 16 K core memory (Goncz 1974a). The digitization of the large number of seismograms required by this study was expedited by a computer-assisted digitizing technique using on-site peripheral devices with the same computer (Goncz 1974b).

Group velocities were inferred from contour plots of frequency-time analysis (FTAN) of the sums of cross-correlograms (Dziewonksi, Bloch & Landisman (1969) and Levshin, Pisarenko & Pogrebinsky (1972)).

Rayleigh waves

The digitized seismograms of the events listed in Table 1 were cross-correlated in the time domain, and an ensemble of cross-correlograms were aligned to common time lag and summed for each path, after normalization, in order to assign equal weight to each event. Thus, there were nine summed cross-correlograms (SCC). The phase spectrum of the SCC is identical to the phase difference spectrum $\phi_2(T)-\phi_1(T)$ in equation (1) (Landisman, Dziewonski & Satô 1969) for computing phase velocity.

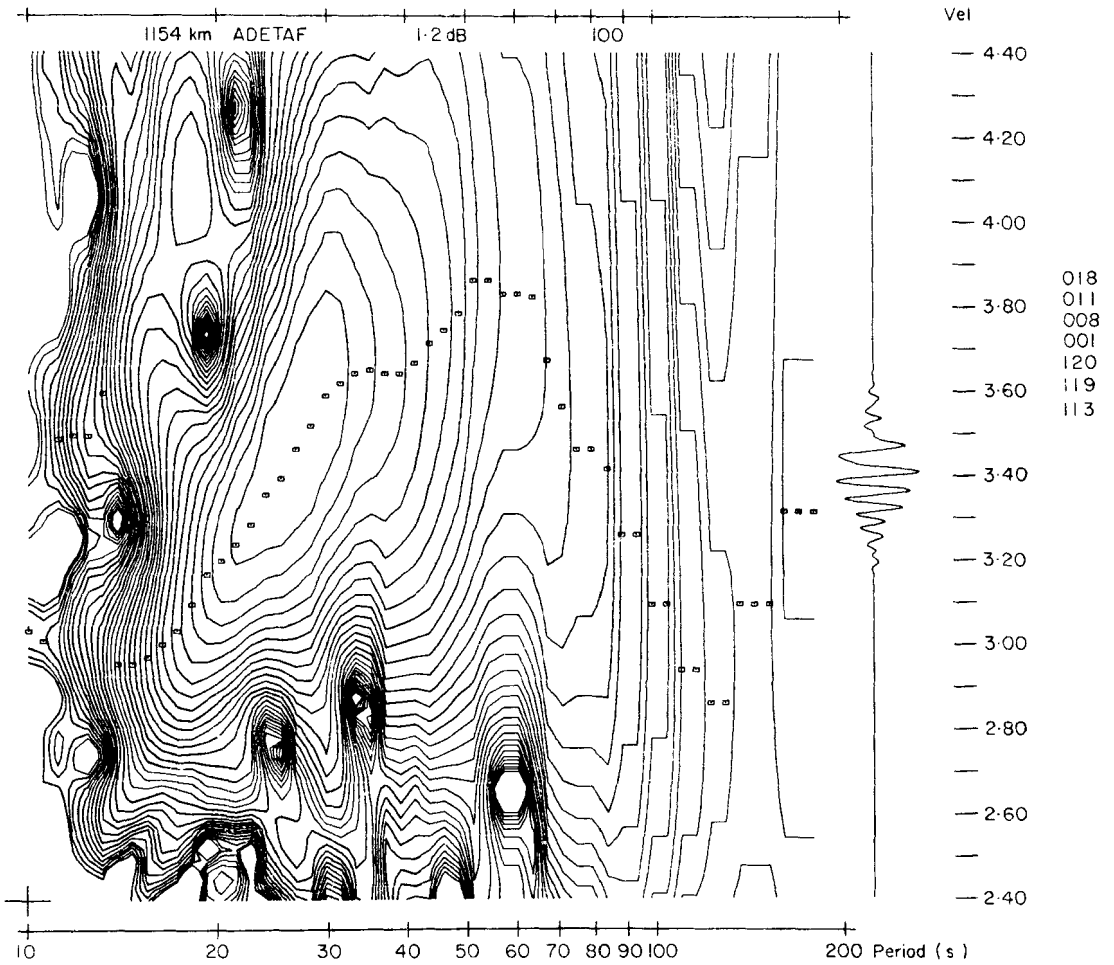

FIG. 2. Contoured frequency-time analysis of sum of cross-correlograms for the ADE–TAU path. The small squares show the maxima at constant periods and they define the ridge crest from which group velocity is inferred.

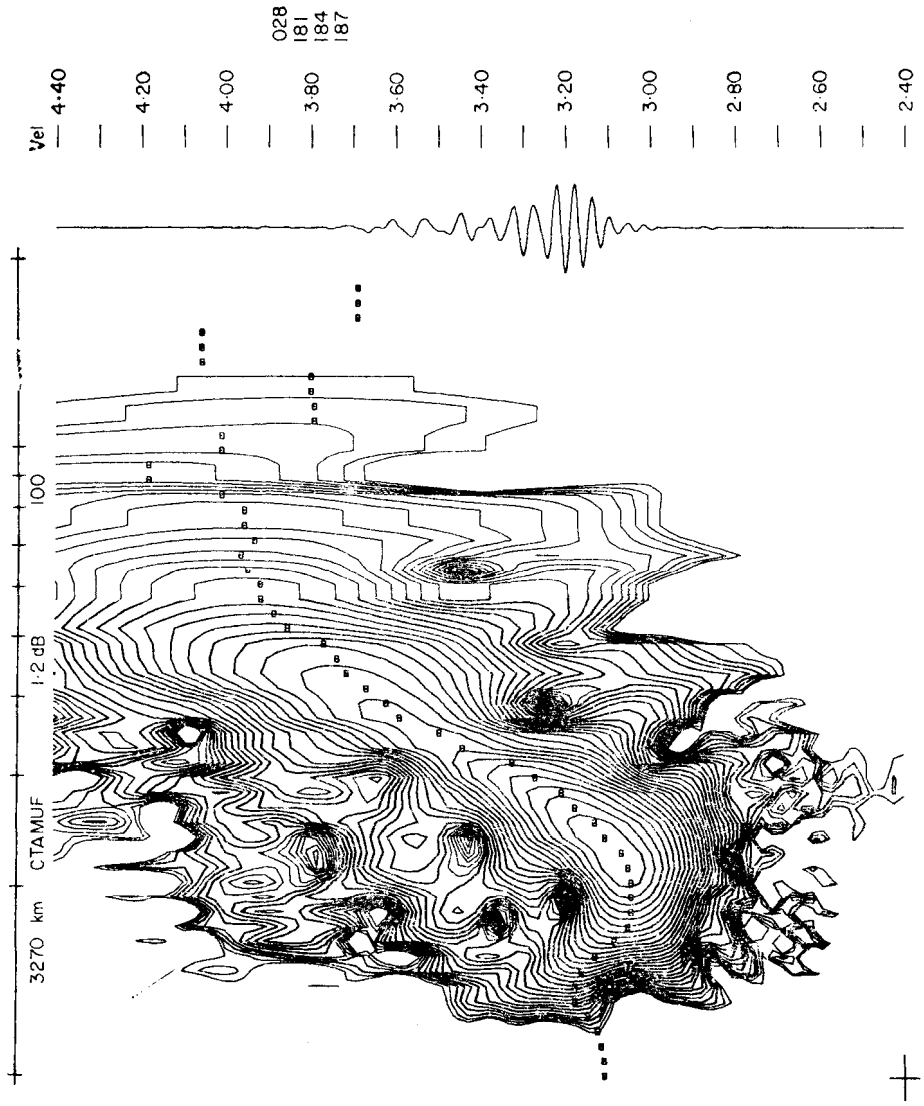

FIG. 3. Contoured frequency-time analysis for sum of cross-correlograms for the path CTA–MUN, also referred to in text as WA1.

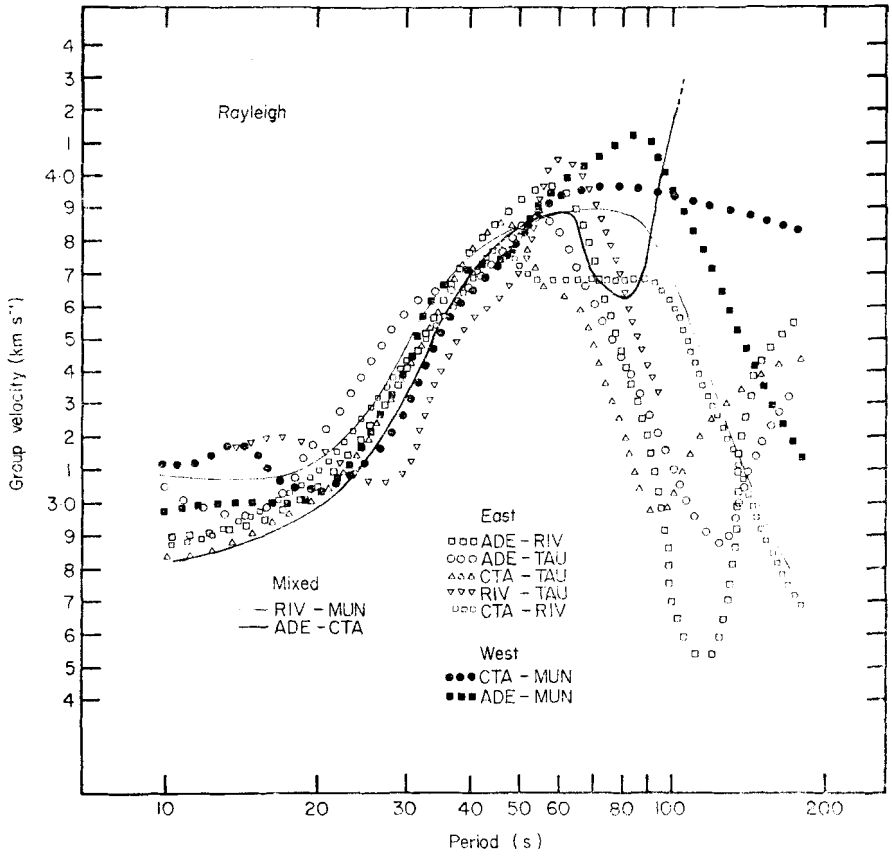

FIG. 4. Rayleigh wave group velocity for nine Australian paths. This information is taken directly from the FTAN plots.

Figs 2 and 3 show the SCC for ADE–TAU and CTA–MUN in the form of a 1024-s time series and the group velocity obtained by frequency-time analysis of the SCC. The output of FTAN is a two-dimensional matrix of signal amplitudes in decibels for 54 log period samples and 85 time samples, the latter having been converted to velocities by the relation $v_\omega(\tau) = D_{12}/\tau$ where τ is time lag. Group velocity is inferred from the contoured FTAN diagram by scanning the FTAN matrix for maxima at constant period (vertical columns). Preservation of the continuity of the ridge crest is used to interpret the complete group velocity curve in the cases where noise may have created a local secondary maximum greater than the maximum associated with the fundamental mode. Fig. 4 shows group velocity curves for the nine paths superimposed for comparison. Note that every group velocity curve reaches a maximum somewhere within the 60- to 100-s period range and there is inverse dispersion beyond the maximum. The group velocity maximum is at a longer period for the paths in western–central Australia –CTA–MUN and ADE–MUN, than the maximum for the paths situated in eastern Australia –ADE–RIV, ADE–TAU, CTA–TAU, RIV–TAU and CTA–RIV. The group velocity curves for eastern Australian paths consistently show a tendency to possess a pronounced minimum at around 120 s, whereas there is no evidence for this tendency in the case of the western–central Australian paths.

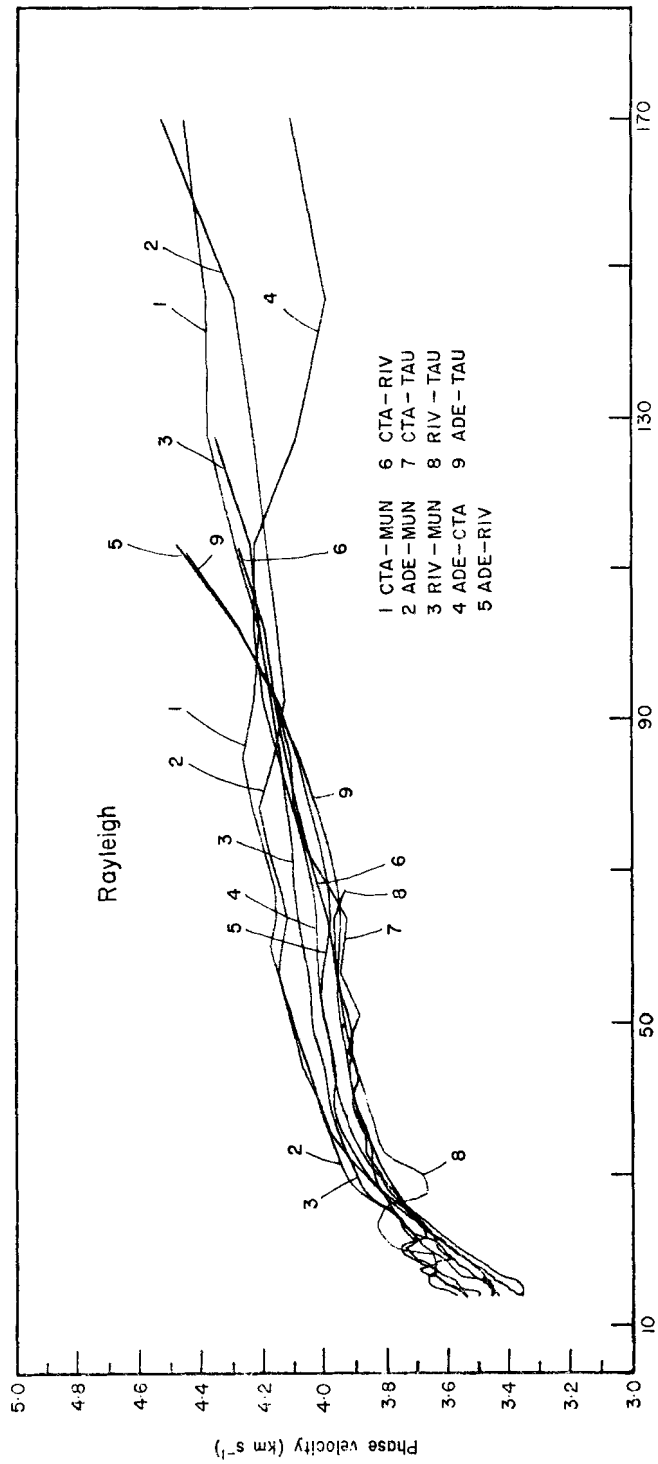

FIG. 5. Rayleigh wave phase velocity for nine Australian paths obtained by Fourier analysis of sum of cross-correlations. No filtering has been used to obtain these results.

Phase velocity curves for the nine paths, obtained by Fourier analysis of the SCCs are shown in Fig. 5, where they are superimposed for comparison. Since no filtering other than a group velocity window between 2·0 and 5·0 km s^{-1} has been applied to the SCC, this set of phase velocity curves represents unbiased measurements.

Whilst there is still residual scatter in these phase velocity curves, a systematic increase in Rayleigh wave phase velocity can be seen between the curves for east Australia and those for the shield region in western–central Australia. In the period range 30–70 s, above the 'knees' of the curves, the phase velocities for the three paths involving Mundaring are about 0·2 km s^{-1} greater than those for the six paths located in eastern Australia. The composite path RIV–MUN appears to be an average of the lower eastern velocity and the higher western velocity. There is some indication that all the nine phase velocity curves tend to merge to a common value of 4·15 km s^{-1} at a period of 100 s.

Close inspection of the phase velocity curves shown in Fig. 5 suggests that the six eastern Australia paths might be further subdivided into two groups. The velocities for the three paths that involve TAU (7, 8, 9) are less than those for the paths involving ADE (4, 5); the amount of the difference is about 0·06 km s^{-1} between 30- and 60-s period. This observation might be explained by the location of ADE, involving greater penetration into the higher velocity shield area, although definite conclusions are hampered by low geographical resolution of the shield boundary and residual uncertainty in the phase velocity curves.

These results differ significantly from the Rayleigh wave phase velocities for the same nine paths obtained by Thomas (1969), who reported 'except where the refraction effects mentioned above are suspected, the results indicate a high degree of uniformity throughout the continent'. Thomas used a modified peak and trough method in conjunction with polynomial smoothing of the discrete phase velocities obtained thereby, and one would expect that this would not be as successful in discriminating phase velocity from signals observed in a noisy environment.

Comparison of the phase velocities shown in Fig. 5 with Knopoff's (1972) Fig. 7, which shows Rayleigh wave phase velocities for 'standard' regions of the world, indicates that the paths CTA–MUN and ADE–MUN are typical of the dispersion observed for shield areas; and the paths CTA–ADE, ADE–RIV, CTA–RIV, CTA–TAU, RIV–TAU and ADE–TAU correspond to 'aseismic platforms'. Knopoff shows shield regions with Rayleigh wave phase velocities about 0·2 km s^{-1} higher than aseismic regions in the period range 30–80 s. The two sets of Australian phase velocity curves agree with this, but appear to merge to a common value of about 4·15 km s^{-1} at about 100-s period, whereas Knopoff (1972) indicates complete separation of shield and aseismic phase velocity curves at this period.

Further signal averaging

Noise reduction, signal enhancement and a linear, unbiased average of all information available for a path are obtained by summing the cross-correlograms of seismograms. It is quite probable that further improvement of these results, particularly in reducing the uncertainty of information at longer periods, would be obtained by increasing the number of events included in the SCC for each path; but a much larger quantity of data would probably be required to achieve a significant improvement.

Further signal averaging can be carried out at this stage by averaging the results of the paths common to the two regions discussed in the preceding section. The SCCs for two or more paths cannot be directly added if the path lengths are different, but signal averaging can be performed by summing the appropriate FTAN matrices

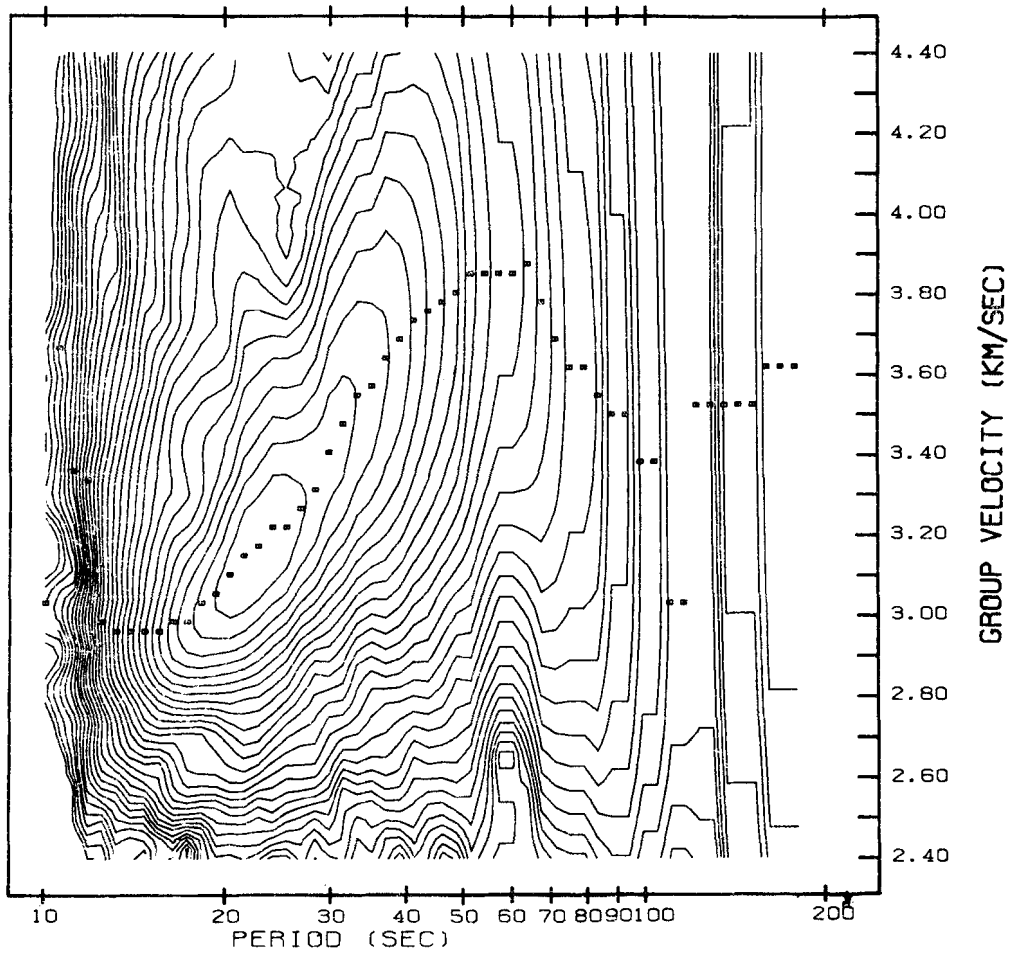

FIG. 6. Group velocity for eastern Australia EA1 after further signal averaging by adding the FTAN matrixes for ADE-TAU, CTA-TAU, ADE-RIV, CTA-RIV and RIV-TAU.

point by point, which is equivalent to averaging group velocities by regions. It is important to consider this approach because, if the difference in group velocity between the two regions can be established, it is equivalent to a 'magnified' picture of the differences in phase velocity.

Therefore, the five FTAN matrices for the eastern Australia paths (CTA–RIV, CTA–TAU, ADE–RIV, ADE–TAU and RIV–TAU) were added point by point, and the resulting contoured plot labelled EA1 is shown in Fig. 6. The group velocity ridge crest is now more coherent than in any of the individual SCCs. The group velocity drops very rapidly for periods greater than 50 s to a minimum value of about 3·0 km s^{-1}. Although the signal level at periods greater than 50 s is low and the actual value of the group velocity at the minimum is subject to large errors, there is no doubt about the steepness of the decrease between 50- and 80-s periods.

For the East Australian paths, the curves for ADE–RIV, ADE–TAU and CTA–TAU are reasonably self-consistent in that they all show a dip in group velocity at about 120-s period followed by a systematic increase at longer periods. The group velocities at periods longer than 100 s for the RIV–TAU path are too scattered to

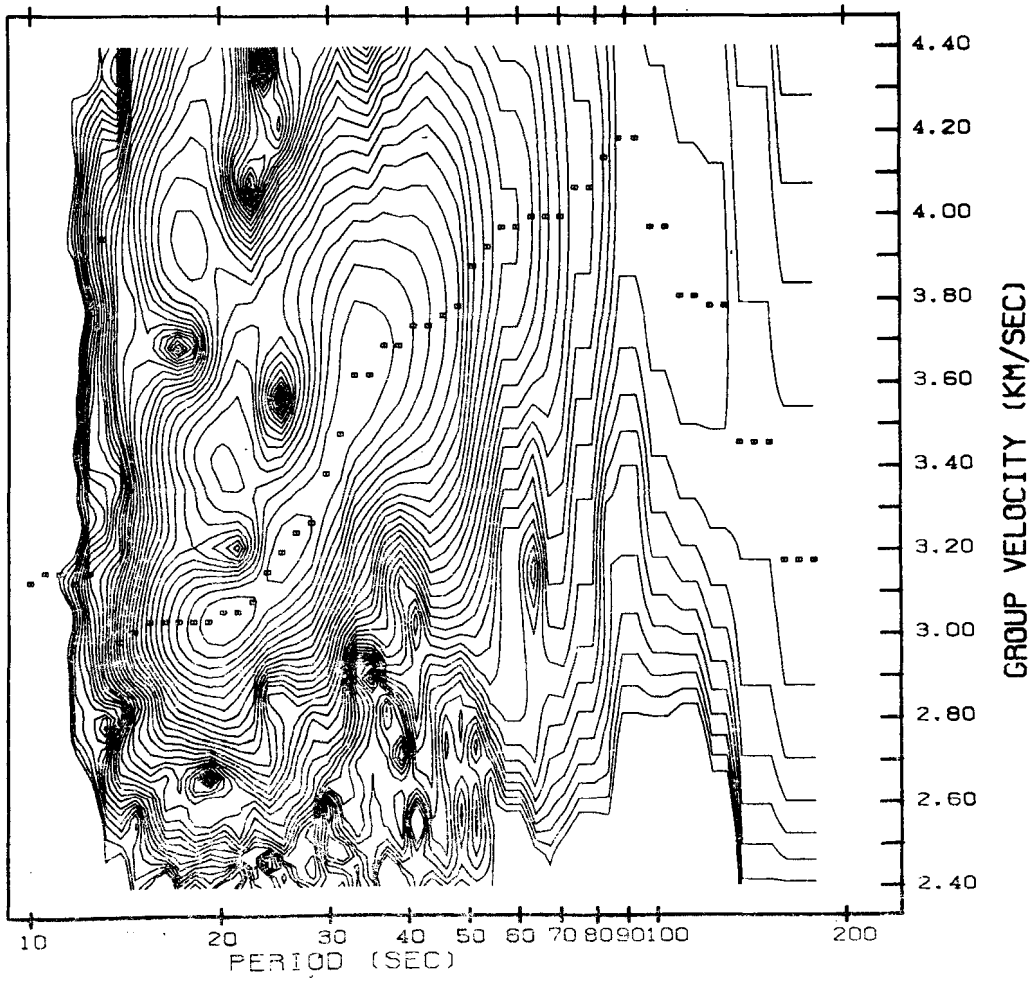

FIG. 7. velocity for Group western Australia WA2 after further signal averaging by adding together the FTAN matrices for CTA-MUN and ADE-MUN.

allow meaningful interpretation. CTA–RIV, on the other hand, shows a steady decrease in group velocity from about 100 s. Although there is no *a priori* reason for discarding the data from this path, it may be considered suspect because of (a) lack of consistency with other paths, and (b) low group velocities at periods beyond 150 s, which (as will be seen) are inconsistent with the results of other workers. For this reason another summation, EA2, of the FTAN matrices for only ADE–RIV, ADE–TAU and CTA–TAU was made. Group velocities for EA1 and EA2 are compared in Fig. 8.

Signal averaging in this manner trades-off geographical resolution in the hope of achieving higher precision as well as extending group velocity information to longer periods.

Of the two paths involving Mundaring, CTA–MUN is an undoubted ' pure shield ' path, whereas ADE–MUN incorporates the edge of the continental shelf for a large proportion of its length (see Fig. 1). Interference problems were encountered at shorter periods due to a multi-path effect in this region. For this reason the FTAN plot for CTA–MUN (Fig. 3) is considered separately and hereafter is referred to

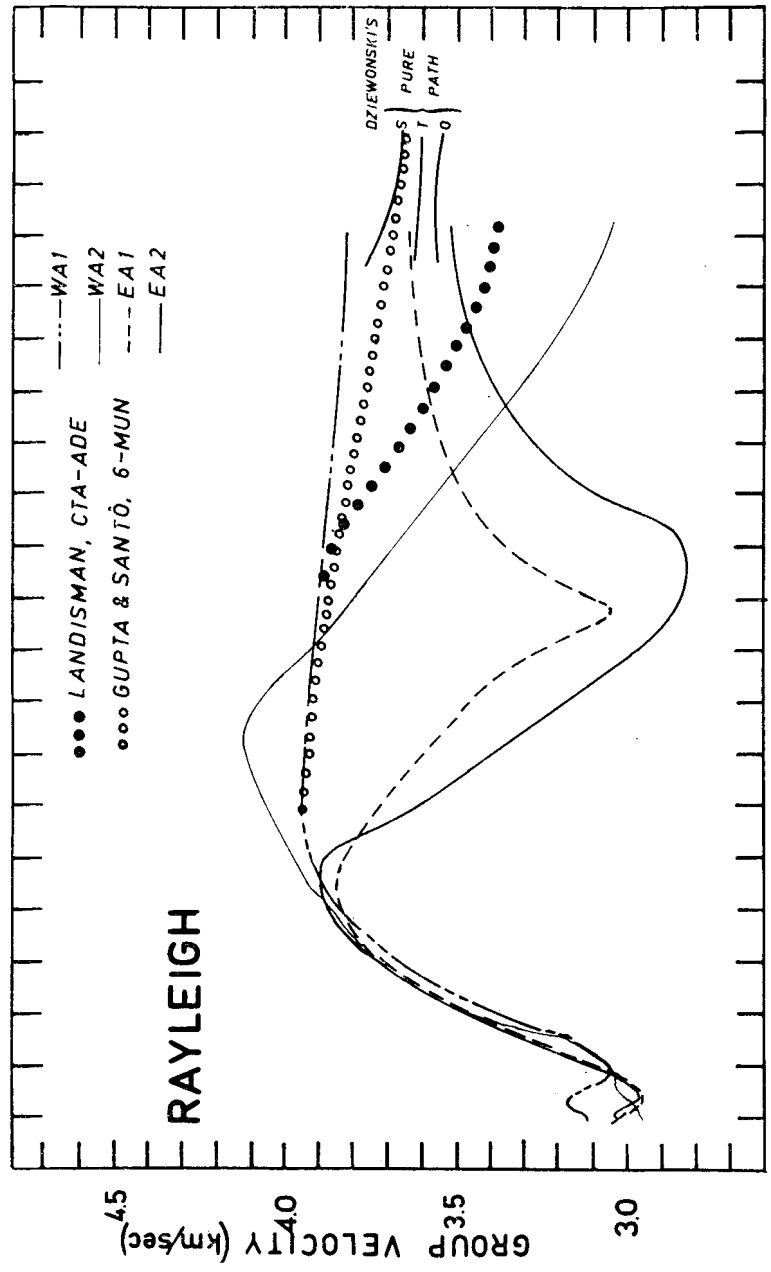

FIG. 8. Group velocity curves for Australia plotted against a linear period axis. Comparison with data from Landisman *et al.*, and word-circling waves by Dziewonski; Gupta and Santò.

as WA1. The label WA2 refers to the group velocity inferred from the contoured matrix (Fig. 7) obtained by summing the FTAN matrices for the paths CTA–MUN and ADE–MUN, point by point.

As a result of this additional signal averaging, the contour diagrams of group velocity displayed in Figs 6 and 7 show further improvement in the coherence of contours, both to longer periods and to shorter periods. It is possible to discern a ridge crest to a period as short as 10 s, although the ridge crest at shorter periods may not coincide with the maxima at constant period indicated by small squares on the contour diagrams. These contour diagrams show that group velocity in eastern Australia has a maximum at a shorter period than group velocity in western–central Australia. The magnitude of the second derivative of the group velocity curve for eastern Australia is greater than that for western–central Australia. This observation proved to be a powerful computable discriminant for testing models in Monte Carlo inversion.

At longer periods the group velocity contour diagrams deteriorate, for a number of reasons. The signal strength becomes progressively weaker at long periods, an indirect consequence of the inability to make use of the strong mantle waves generated by great earthquakes in the two-station direct observation method. In consequence local maxima are being estimated in a two-dimensional region of extremely small gradients; this situation is further degraded by the low resolution of FTAN which diffuses the signal both in time and in frequency.

These observations can be seen more clearly in Fig. 8 where the group velocity curves are plotted against a linear period scale to avoid the compression of a logarithmic abscissa. It is apparent that little regional difference in group velocity exists over the period range from 10 to 50 s. This observation indicates great uniformity in the composition and depth of the crust over the whole continent of Australia.

The results at periods longer than 100 s must be treated with caution, for the reasons already given. Nevertheless, the results graphed in Fig. 8 show that group velocities of mantle waves generated by earthquakes of moderate magnitude having periods up to 200 s can be measured by the two-station method within specific geographical regions, as distinct from deriving this information from world-circling waves.

For comparison, the results of three surface wave studies have been included in Fig. 8: (1) Dziewonski's (1971) pure path data, which extend to periods as short as 150 s, (2) Gupta & Santô's (1973) world average data, which extend down to 90 s, and (3) a group velocity curve obtained by differentiating the phase velocity curve obtained by Landisman *et al.* (1969) for the CTA–ADE path. Dziewonski's data are representative of Fourier analysis of world-circling waves; his data agree closely with other free oscillation studies and are not expected to change significantly as new information becomes available. Gupta & Santô attempted to extend the analysis of world-circling waves to shorter period by careful selection of seismograms that showed inverse dispersion sufficiently clearly to permit the use of the peak and trough method. The Landisman *et al.* group velocity curve in Fig. 8 was obtained by graphical differentiation of the published phase velocity curve according to the equation

$$U(T) = \frac{c(T)}{1 + \frac{T}{c}\frac{dc}{dT}}. \tag{2}$$

The group velocity curve derived from Landisman *et al.* is a measurement of group velocity in a limited geographical area. The data of Dziewonski, and of Gupta & Santô constitute regional group velocity deduced from surface waves that have travelled

completely around the Earth. The WA2 curve is not congruent with the 'shield' curve of Dziewonski in the range 150–200 s, although it is less discrepant with the Landisman *et al.* curve. WA1, on the other hand, agrees well with both the Dziewonski and the Gupta & Santô results. Curves EA1 and EA2 both join reasonably well with Dziewonski's tectonic curve at about 180 s. Even at these extended periods, then, the present data are not necessarily in conflict with the data arrived at by other methods, and may be taken to confirm that systematic differences exist between group velocities for shield and tectonic regions in the period range 100–200 s. The suggestion of a dip in group velocity at about 120 s across tectonic regions certainly warrants further investigation.

At periods shorter than 100 s the group velocity measurements are less subject to error and, when the large number of events that have been included by a linear averaging process is taken into account, considerable confidence can be placed in the measurements at periods less than 100 s. The profiles of group velocity must be evidence of systematic changes in the characteristics of the low velocity channel.

Integration of group velocity

Pilant & Knopoff (1970) pointed out that an inversion of group velocity data will possess an additional degree of non-uniqueness compared to an inversion of phase velocity data. This follows from the fact that group velocity is a derivative function of phase velocity, and therefore there is an infinite number of phase velocity curves which, upon differentiation, yield the same group velocity curve. Additional information, or constraints, can be used to associate a unique phase velocity curve with a given group velocity curve, over a specified band of frequencies.

The unsmoothed phase velocity curves shown in Fig. 5, obtained from unfiltered Fourier analysis of sums of cross-correlograms, are not yet suitable for inversion. They must be smoothed. Usual smoothing techniques such as moving average or polynomial fitting do not add information to the data. Since group velocity measurements are obtained by a different process they contain additional information about the slope of the phase velocity curve. In the present study, the combination of (1) summing cross-correlograms from an ensemble of events, and (2) adding their FTAN matrices has produced group velocity curves than can be integrated, and therefore integration is a preferred method of smoothing.

Phase velocity curves were derived from the four regional group velocity curves by numerical integration according to the equation

$$c(\omega) = \frac{\omega}{\int_{\omega_1}^{\omega} \frac{d\omega}{U(\omega)} + k(\omega_1)} \tag{3}$$

which follows from the well-known relation $U(\omega) = d\omega/dk$.

Since the wave number $k(\omega_1)$ at the longest period of interest is not known accurately, an estimate of its value was made in the following manner. Each group velocity curve was numerically integrated with $k(\omega_1)$ varied in steps of $0{\cdot}0001\ \pi$ s km^{-1} in successive integrations. A family of phase velocity curves was obtained, and an example, WA2, is shown in Fig. 9. Note that each of these phase velocity curves has the same group velocity curve. This family of curves was compared with the CTA–MUN and ADE–MUN phase velocity curves in Fig. 5 in the period range 40–80 s, and the value for $k(\omega_1)$ giving the best fit in this period range was found by visual interpolation. Equation (3) was then integrated with this value for $k(\omega_1)$ to obtain the phase velocity curve WA2 shown in Fig. 10. Proceeding in the same manner,

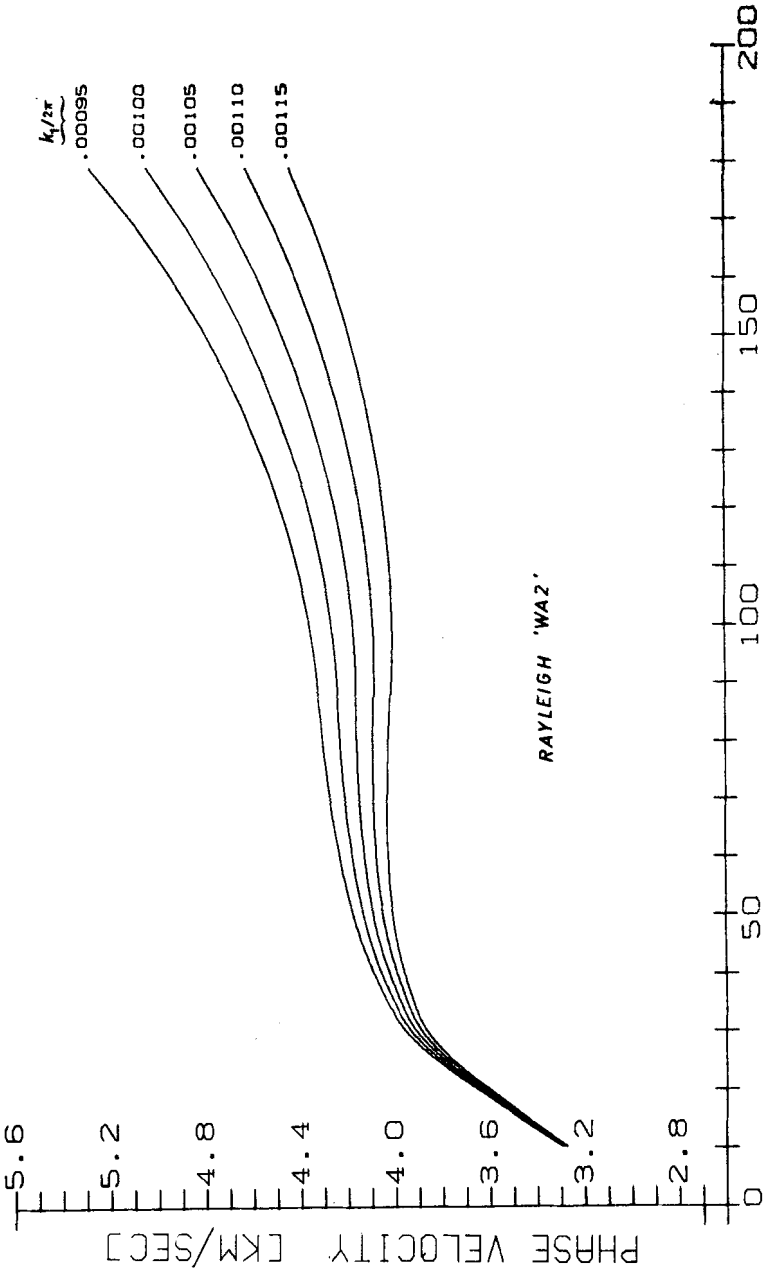

FIG. 9. Family of phase velocity curves obtained by integrating the group velocity curve WA2. Wave number at 183 s is not known accurately. This family of curves was visually compared with Fig. 5 to obtain a value for $k(\omega_1)$.

regional phase velocity curves for WA1 and EA1 were obtained by integrating group velocity and are shown also in Fig. 10. Significant features of this presentation are:

(1) Between 40- and 80-s period the phase velocities in ' West Australia ' are about 0·2 km s^{-1} higher than those in ' East Australia '.

(2) The curves merge to a common value, 4·15 km s^{-1}, at 110-s period.

(3) In the period range 10–25 s the phase velocities for East and West Australia are nearly the same, there being less than 0·05 km s^{-1} difference.

Comments (1) and (2) are concordant with the regional differences found for group velocity and are also concordant with the observations made on the unsmoothed phase velocities of Fig. 5. Comment (3) cannot be applied to the unsmoothed phase velocities determined from Fourier analysis of summed cross-correlations, which show considerable scatter at short periods. It can be concluded that FTAN summation of paths of different length followed by integration of group velocity is an effective way of obtaining a smooth phase velocity curve from noisy data.

Fig. 10 shows three phase velocity curves obtained by integrating group velocity: WA1 (this is the single path CTA–MUN), WA2 (combined FTAN matrices for CTA–MUN and ADE–MUN), and EA1 (FTAN matrices for all six East paths). One more phase velocity curve was considered, EA2, a selection of certain eastern paths, characterized by a broader and lower dip in group velocity than EA1 exhibits. It was found impossible to maintain a reasonable wave number (or phase velocity) at the longest period and at the same time maintain agreement with Fourier phase velocities in the 40- to 80-s range. For this reason, EA2 has not been included in Fig. 10. This observation indicates that the group velocity minimum between 100 and 200 s cannot in reality be as pronounced as shown in EA2. The FLO–GOL phase velocity curve is taken from Knopoff (1972). It was used for the inversion of

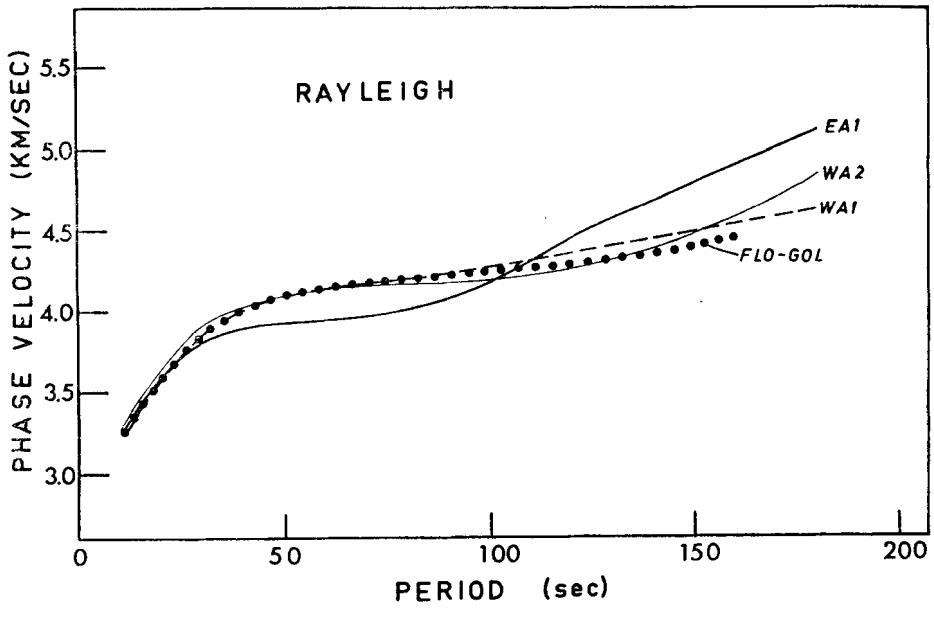

FIG. 10. Regional Rayleigh wave phase velocity curves for Australia obtained by integration of group velocity curves.

shield regions by Knopoff (1972) as it is typical of Rayleigh wave phase velocity observed in shield areas.

Love waves

The method used to obtain Rayleigh wave phase velocity curves for East and West Australia can be summarized in four stages:

(1) All available cross-correlograms common to one path are summed.

(2) Frequency-time analysis contour plots are prepared from these sums of cross-correlograms.

(3) FTAN matrices for neighbouring paths that exhibit similar phase velocity curves are added together point by point.

(4) A phase velocity curve is obtained by integration of the group velocity curve inferred from the last step.

This four-stage process appears to have been successful in extending the range of dispersion information obtained in the two-station method to about 200 s, although uncertainties in the data still exist at longer periods.* An attempt was made to apply the same processing techniques to obtain extended Love wave dispersion information, also.

The measurement of Love wave dispersion may be complicated by interference between the higher modes and the fundamental mode. Thatcher & Brune (1969) showed that for many Earth structures the fundamental, first and second higher mode group velocities were so close together that these modes do not separate in time on the seismogram. A beat phenomenon between the modes occurs, with a beat wave length of the order of 1000–2000 km. Rapid fluctuations in apparent phase velocity would be expected if the recording station were located in the vicinity of a beat mode. They suggest that such rapid phase velocity fluctuations have not been reported because such results would have been judged to be of poor quality and would have been discarded before final reporting.

In a companion paper, Boore (1969) concluded that ' the first higher mode can be an important contaminant of the fundamental (Love) mode, but that interstation phase velocities measured over an ensemble of events should show scatter but no strong bias '. His analysis of the problem showed that phase velocities for the fundamental mode perturbed by the higher mode would oscillate about the unperturbed value and that the length of the oscillation would increase with longer periods.

In the present study no attempt at pre-selection of Love wave data has been made; all readable horizontal seismograms were cross-correlated and included in the sum for the appropriate path. The digitized seismograms were combined to obtain transverse ground motion. The sums of cross-correlograms so obtained for the nine paths were Fourier analysed to obtain a preliminary phase velocity curve for each path and these results are shown in Fig. 11. The FTAN contour plots for two of the nine sums of cross-correlograms are shown in Figs 12 and 13.

The Love wave FTAN plots derived from stacking cross-correlograms show some signal–noise ratio enhancement when compared with the FTAN contour plots of individual events, but it is obvious that more signal enhancement is needed if Love wave group velocity is to be measured with the same reliability as had been achieved with Rayleigh wave group velocity. The plots are highly disorganized, but it is not

* This method of processing achieves an increase SNR but sacrifices an estimation of error bounds. A similar situation occurs in the vectorial combination of data to enhance specific eigenperiods of vibration of the Earth (Mendiguren 1973).

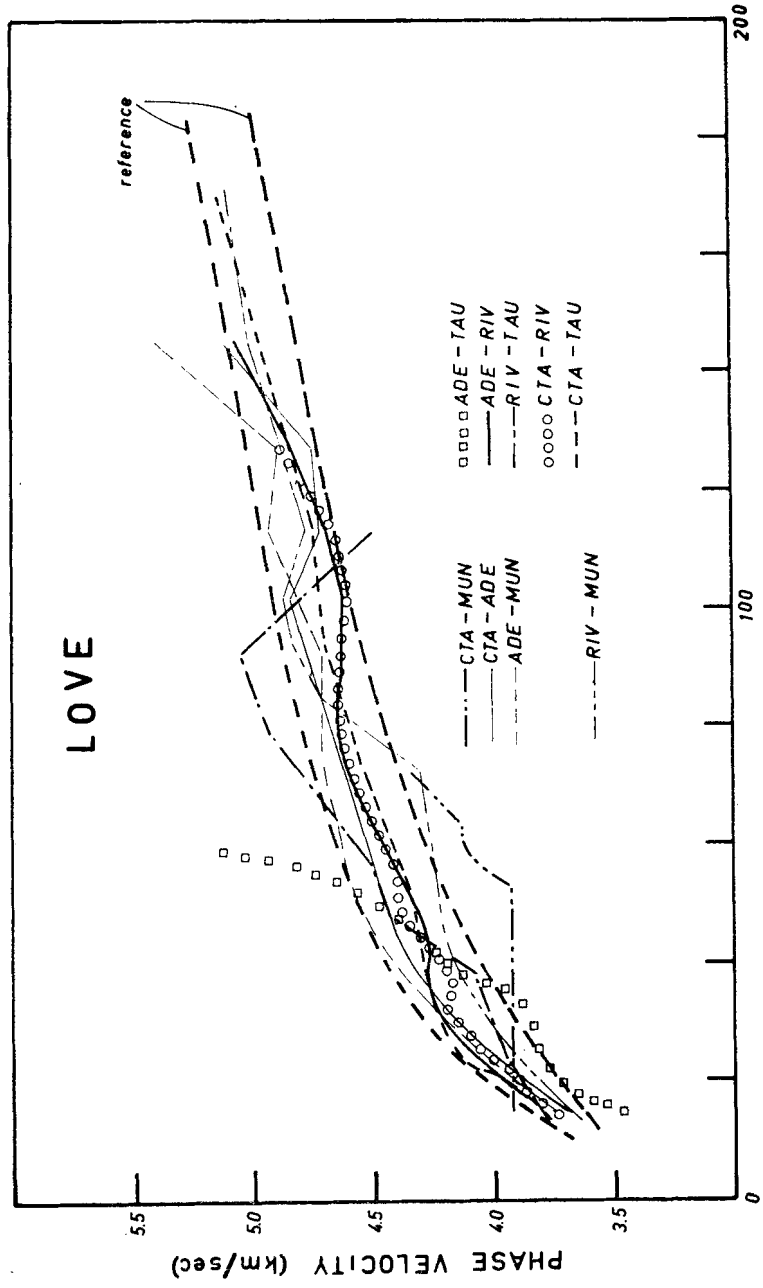

FIG. 11. Love wave phase velocities obtained by Fourier analysis of sums of cross-correlations. See section on Love waves for explanation of scatter.

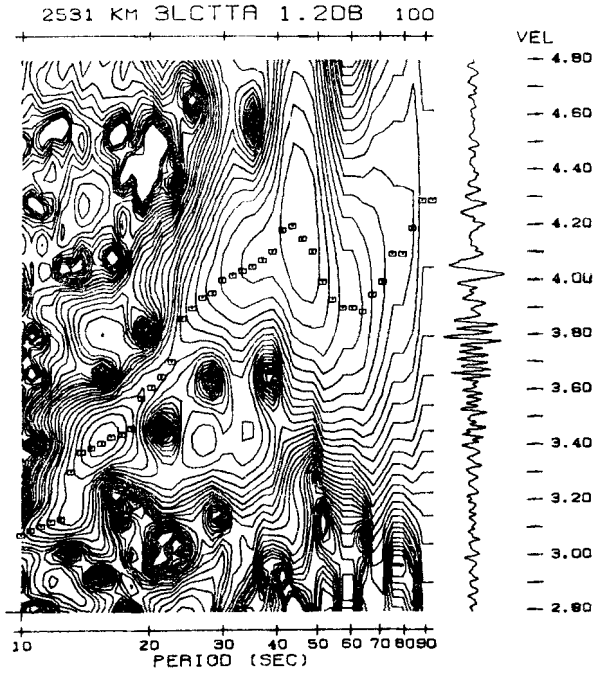

FIG. 12. Love wave group velocity from sum of two cross-correlograms for the path CTA-TAU.

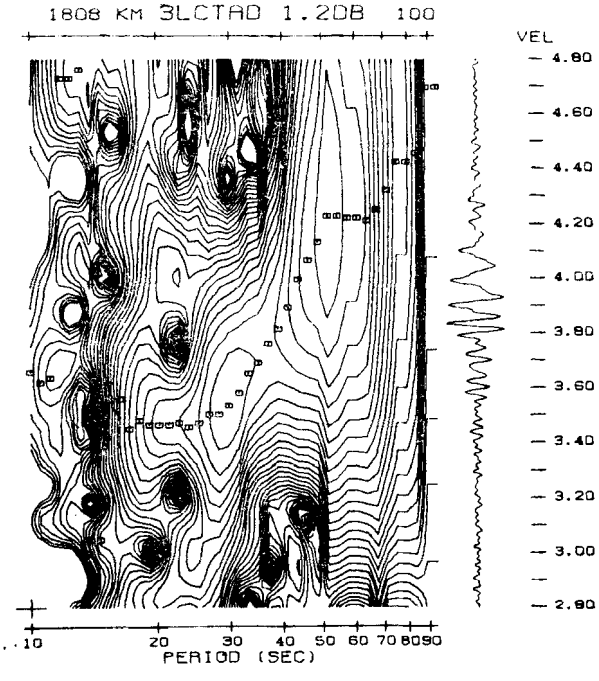

Fig. 13. Love wave group velocity from sum of three cross-correlograms for the path CTA–ADE

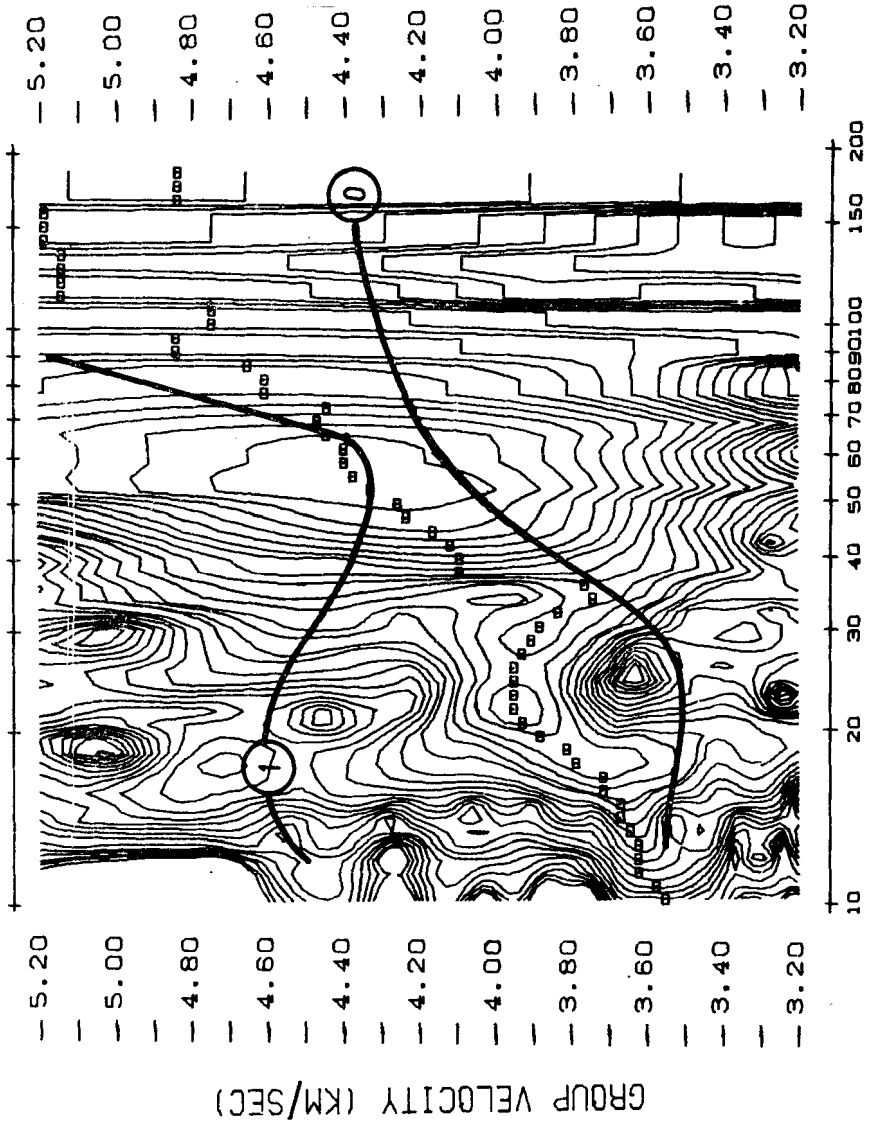

FIG. 14. Love wave group velocity for 'West' Australia after further signal averaging by adding the FTAN matrices for CTA–MUN and ADE–MUN. 0 indicates the Love wave fundamental mode from a 'West' Monte Carlo model and 1 indicates the first higher Love mode. *cf* Goncz & Cleary, in preparation.

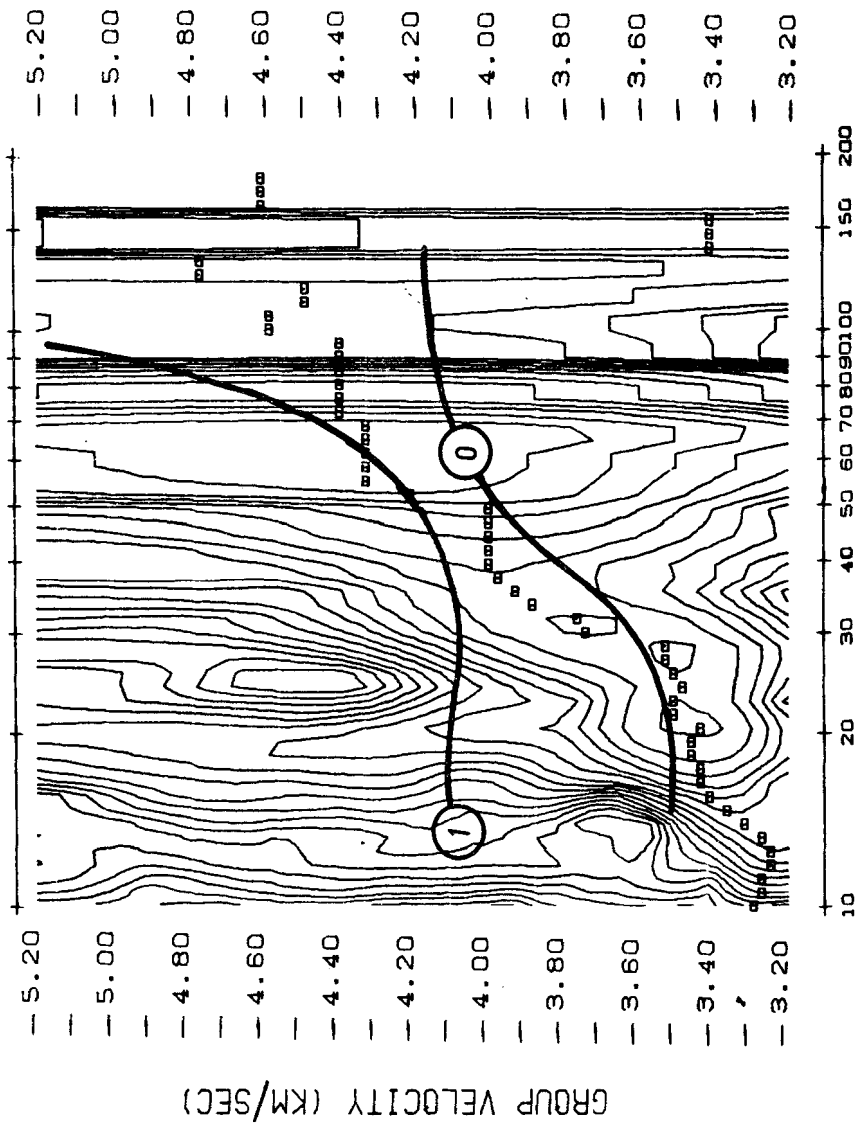

FIG. 15. Love wave group velocity for 'East' Australia after further signal averaging by adding the FTAN matrices for ADE–TAU, CTA–TAU, ADE–RIV, CTA–RIV, and RIV-TAU. Fundamental and first higher Love wave models shown were calculated for an 'East' Monte Carlo model, *cf.* Goncz & Cleary (1975).

clear whether the source of the disorganization is incoherent noise, incomplete elimination of Rayleigh wave motion or inability to resolve the fundamental Love wave mode from higher modes.

Although the Love wave phase velocity curves shown in Fig. 11 indicate the need for further signal enhancement, we can make some useful observations about this data as presented. Oscillations of the phase velocity curve about its unperturbed value, predicted by Boore (1969), are suggested by the behaviour of the phase velocity curves RIV–MUN, ADE–RIV, and CTA–RIV. The behaviour of the curves for RIV–TAU, CTA–MUN and ADE–TAU may be similar to the rapid phase fluctuations predicted by Thatcher & Brune (1969), which are not apparent in the six other phase curves. It is significant that the phase velocities for CTA–MUN, CTA–ADE and ADE–MUN, in the period range 40–100 s, are higher than for the other paths, indicating a higher shear wave velocity structure in western Australia than in eastern Australia, in agreement with the results described previously for Rayleigh waves.

In an attempt to achieve better definition of Love wave group velocities the same philosophy used for Rayleigh waves was applied to this part of the study by summing the Love wave FTAN matrices for West Australia (CTA–MUN and ADE–MUN) and for East Australia (ADE–RIV, ADE–TAU, CTA–RIV, CTA–TAU and RIV–TAU). The results of these summations are shown in Figs 14 and 15. Considerable improvement in the coherence of the ridge crest has been obtained in both cases. The heavy lines on these two figures are theoretical Love wave group velocities for the fundamental and first higher mode for earth models obtained in an inversion study described fully in a companion paper (Goncz & Cleary). Since the ridge crest obtained by FTAN analysis of real data lies between these two curves, it can be concluded, in part at least, that the fundamental and first higher Love mode are too close together to be fully resolved by FTAN. This conclusion is supported by the negative results of an attempt to integrate the measured Love wave group velocity curves to obtain a fit to the Love wave phase velocities of Fig. 11, whereas this could be done for Rayleigh waves.

The obvious conclusion is that, until methods are found that will permit the higher modes to be resolved from the fundamental mode, any Love wave group velocity information obtained by FTAN must be considered to be biased toward higher values by an unknown amount. However, it appears that averaging an ensemble of events via the ' sum of cross-correlations ' method combined with Fourier analysis does give reasonably accurate fundamental Love wave phase velocities, for individual paths.

Discussion

Because Australia is an 'island continent' the surface waves that are used to investigate the dispersion across Australia must cross the continental–oceanic boundary at some point, and as a consequence, the difficulties associated with refraction effects are unavoidable. The consequence of wave refraction is that energy is transmitted and recorded at one of the two-station pair by a path other than the greater circle between the two stations. As a result, the phase function measured by the cross-correlogram is perturbed.

The effect of the perturbation can be reduced by using an ensemble of events with varying epicentral distances, and probably more effectively by including within the sum of cross-correlograms, an approximately equal number of events whose waves enter the two-station path from either side.

For Rayleigh waves, this approach appears to have been successful for the ADE–TAU path (Fig. 2) in which case there were four events whose waves entered the path through TAU and two events whose waves entered the path through ADE.

Notice that the group velocity FTAN contour plot of the SCC for this path in Fig. 3 is quite coherent and noise free. However, a similar situation for the RIV–TAU path, where three events on either side of the path were used, was not at all successful. The reason for this difference in results is not obvious.

Since group velocity is a more sensitive measurement of dispersion than phase velocity, the feasibility of the pronounced dip exhibited by Rayleigh wave group velocity for the paths in eastern Australia will be examined. A summary of pertinent information is presented to determine if this unexpected behaviour of group velocity might be real.

Firstly, two paths, ADE–MUN and CTA–MUN, which are located to the west of the boundary defined by the CTA–ADE path (see map, Fig. 1), could be more-or-less successfully analysed by the cross-correlation method to obtain reasonable phase velocities to periods as long as 170 s. On the other hand, these figures also show that this type of analysis becomes unreliable at 100 s or less for the six paths located to the east of this line. The analysis for the mixed path RIV–MUN, which traverses both regions, appears satisfactory to 130 s. These observations lend confidence to the ability of the sum of cross-correlations method to enhance signal strength in the 100- to 200-s range, and suggest that there is something unusual about Rayleigh wave propagation in eastern Australia.

Events 4 and 5 are interesting because the same seismograms were used in the analysis of RIV–MUN (East), ADE–MUN (West) and RIV–MUN (traversing both East and West). Using the same surface waves, the latter two paths can be analysed to longer periods than the RIV–ADE path, which is contained entirely in eastern Australia. This tends to rule out the possibility that a loss of long period signal strength associated with the events used in the analysis of eastern Australia might be responsible for the unusual dispersion observed there at periods between 100 and 200 s. The CTA–ADE path, which skirts the shield boundary, was successfully analysed to long periods, but note that its group velocity tends to drop below that of the pure shield path CTA–MUN, as though partially influenced by the peculiarities of the eastern region. (This is confirmed also by Landisman's results shown in Fig. 8.)

Fig. 5 shows that the phase velocity curves for the eastern paths tend to cross the curves for the shield region at about 100 s, and the small amount of information at longer periods than this (see 5, 6 and 9 in Fig. 5) indicates that they continue to remain above the shield curves at longer periods. This tendency is shown clearly in Fig. 10 by the EA1 phase velocity curve. This curve was obtained by integrating the EA1 group velocity curve, and it fits the individual path data, as determined by Fourier analysis of summed cross-correlations, quite well to 110 s.

This reasoning does not directly support the reality of the group velocity dip, but shows that a consistent overall data set is possible. The group velocity results can therefore be tentatively accepted at face value. It remains to be established whether a realistic Earth model can be obtained that fits the observed group velocities.

Fig. 16 shows a three-dimensional representation of the group velocity inferred from the FTAN matrix for the path CTA–MUN. The spectral amplitude axis is linear in this representation rather than in decibels. This type of presentation is useful as an aid in determining whether certain regions of the two-dimensional contours plot are peaks or valleys. The problem of low signal strength at longer periods is partly due to the limited dynamic range of the WWSSN recording instrumentation; that is R_1 from a large, close earthquake is usually off-scale, and cannot be read. Thus, the large signal power associated with large earthquakes cannot be utilized. There is a growing use of digital recording, which is capable of greater dynamic range, and the data bank of the next fifteen years will contain many more seismograms usable in the 100- to 200-s period range. This will permit critical regional group velocity measurements similar to the present study to be made, and these investigations

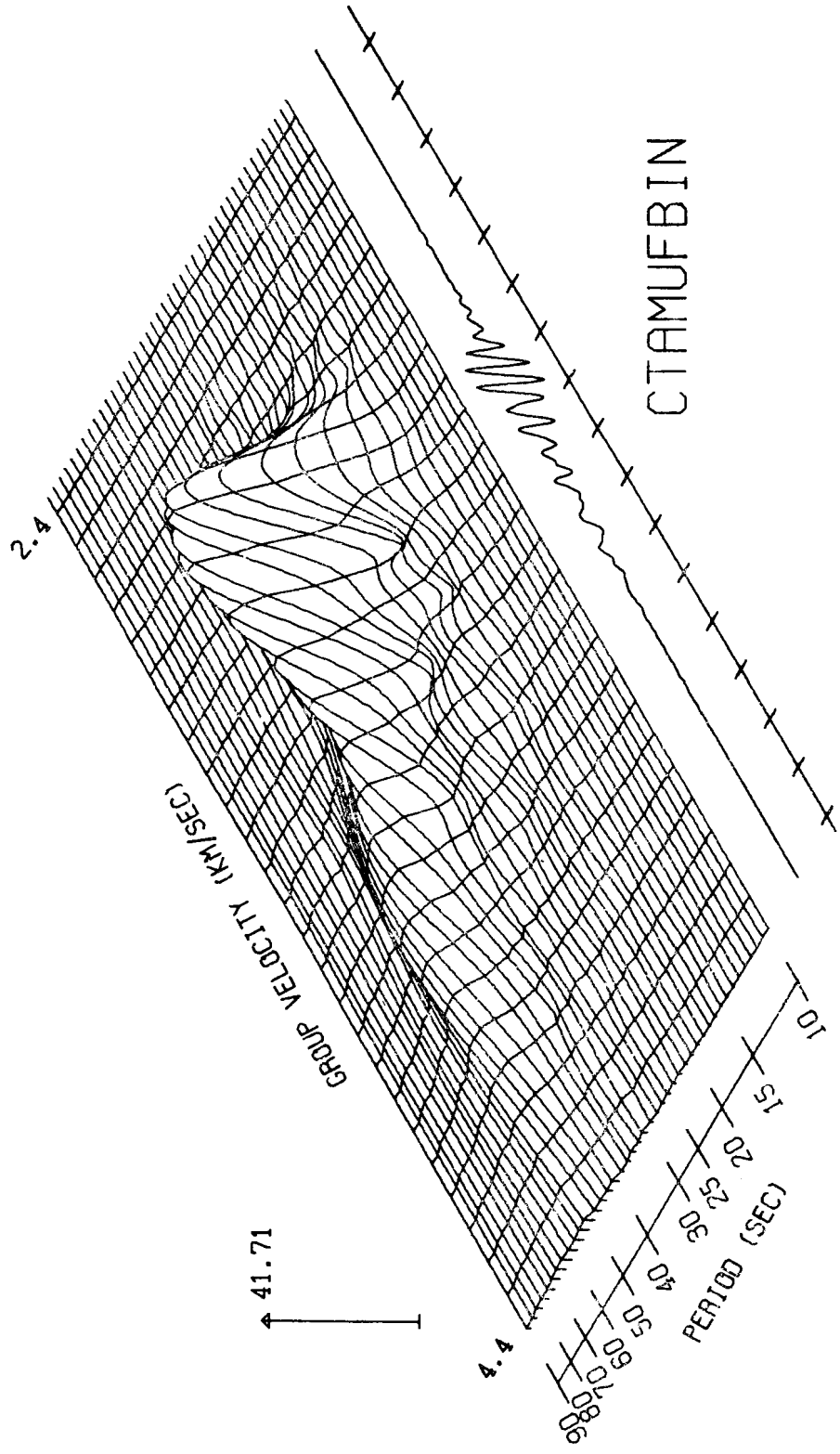

FIG. 16. Three-dimensional representation of the FTAN matrix of the SCC for the path CTA–MUN.

should reveal the differences in upper mantle structure throughout the Earth, beneath well-defined geographical areas.

Acknowledgments

The contour program used in this study was written by Mr J. A. B. Palmer, Division of Computing Research, CSIRO, and we gratefully acknowledge its usefulness. We thank Dr L. Thomas for making available his selection of seismic recordings. We are grateful to Professor S. Alexander for critical comments on this work.

J. H. Goncz:
Research School of Physical Sciences,
The Australian National University.

A. L. Hales and K. J. Muirhead:
Research School of Earth Sciences,
The Australian National University.

References

Bolt, B. A. & Niazi, M., 1964. Dispersion of Rayleigh waves across Australia, *Geophys. J. R. astr. Soc.*, **9,** 21–35.

Boore, D. M., 1969. Effect of higher mode contamination on measured Love wave phase velocities, *J. geophys. Res.*, **74,** 6612–6616.

Dziewonski, A. M., 1971. On regional differences in dispersion of mantle Rayleigh waves, *Geophys. J. R. astr. Soc.*, **22,** 289–325.

Dziewonski, A. M. & Hales, A. L., 1972. Numerical analysis of dispersed seismic waves, *Methods of computational physics*, Vol. 11, 39–85, Academic Press, Inc., New York and London.

Dziewonski, A., Bloch, S. & Landisman, M. 1969. A technique for the analysis of transient seismic signals, *Bull. seism. Soc. Am.*, **59,** 427–444.

Goncz, J. H., 1974a. *Surface wave studies of the Australian upper mantle*, Ph.D. Thesis, The Australian National University, Canberra, A.C.T., Australia.

Goncz, J. H., 1974b. Computer aided digitization of chart records, *J. Phys. E: Sci. Instrum.*, **7,** 20–22.

Goncz, J. H. & Cleary, J. R. Variations in upper mantle structure beneath Australia from surface wave observations *in preparation.*

Gupta, H. K. & Santô, T., 1973. Worldwide investigation of mantle Rayleigh-wave group velocities, *Bull. seism. Soc. Am.*, **63,** 271–281.

Knopoff, L., 1972. Observation and inversion of surface-wave dispersion, A. R. Ritsema (editor), The Upper Mantle, *Tectonophysics*, **13,** (1–4), 497–519.

Landisman, M., Dziewonski, A. & Satô, Y., 1969. Recent improvements in the analysis of surface wave observations, *Geophys. J. R. astr. Soc.*, **17,** 369–403.

Levshin, A. L., Pisarenko, V. F. & Pogrebinsky, G. A., 1972. On a frequency-time analysis of oscillations, *Ann. Geophys.*, **28,** 211–218.

Mendiguren, J. A., 1973. Identification of free oscillation spectral peaks for 1970, July 31, Columbian deep shock using excitation criterion, *Geophys. J. R. astr. Soc.*, **33,** 281–321.

Pilant, W. L. & Knopoff, L., 1970. Inversion of phase and group slowness dispersion, *J. geophys. Res.*, **75,** 2135–2136.

Thatcher, W. & Brune, J. N., 1969. Higher mode interference and observed anomalous apparent Love wave phase velocities, *J. geophys. Res.*, **74,** 6603–6611.

Thomas, L., 1969. Rayleigh wave dispersion in Australia, *Bull. seism. Soc. Am.*, **59,** 167–182.